



## SHORT-STROKE ROTARY APPLICATION OF THE A31315

By David Hunter  
Allegro MicroSystems

### Introduction

This guide is intended to assist the reader in applying the A31315 Samples Programming Software to their short-stroke rotary application, such as a throttle-body, which uses the A31315 Advanced Linear Sensor and a target motion of 0 to 90°. It aims to briefly discuss the magnetic target and instruct the reader on the application of gain and offset, two-point programming, and linearization for the highest level of performance possible.

### Magnetic Target

Magnetic target selection is typically approached with two core requirements: target cost and target field strength. For applications using the A31315, it is preferable that the peak field strength in any one channel reach a minimum of 300 G for overall sensor performance but is not required. This number is blind to material types and air gaps, but cost sensitivities will influence those factors. A neodymium N52 material can produce an excellent field strength for the given size but may cost significantly more than an AlNiCo magnet at a weaker field, requiring a narrower air gap.

For the example in this document, a diametrically polarized N35 magnet of 0.375-inch diameter is used with a 4 mm air gap (reducing the peak field). The sensor is installed on a real throttle body module and is intended to be programmed to linearly output sensed position from 0.5 to 4.5 V.

A simple 1-D linear sensor sensing a rotating diametrically polarized magnet will not receive a linear field proportionate to angle; at best, it will detect a sinusoidal signal. Further, unless every magnet is precisely installed from module to module, the initial angle will be unknown, which means a lookup table mapping of input to output becomes less viable.

The A31315 offers sensing of two axes which—through

the application of an integrated arctangent function via a CORDIC engine—can provide a generalized initial magnetic position. Figure 1 illustrates the ideal case where a magnetic target of 250 G strength travels over 90° from an arbitrary starting point.

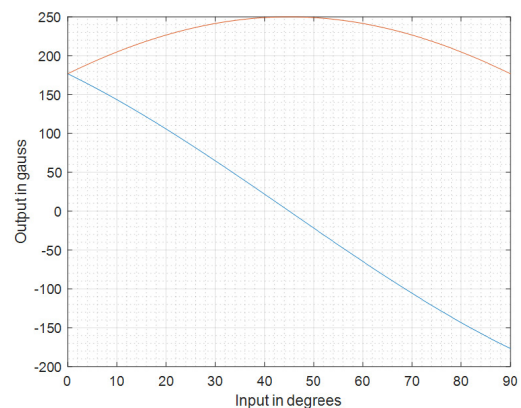


Figure 1: Ideal sensed input of a perfect 250 G magnet.

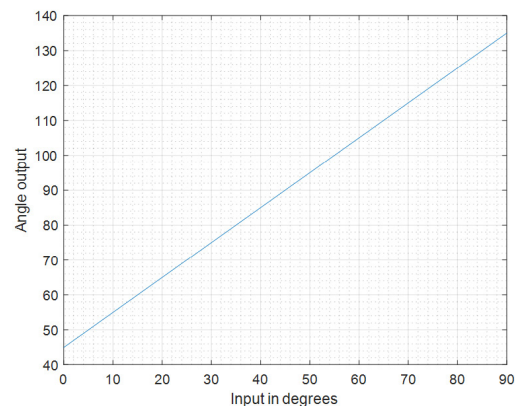


Figure 2: Angle output by CORDIC engine.

In reality, a magnet is an imperfect quantity. Additionally, the position of the sensor once installed is seldom perfectly centered. The result is then measured as shown in Figure 3.

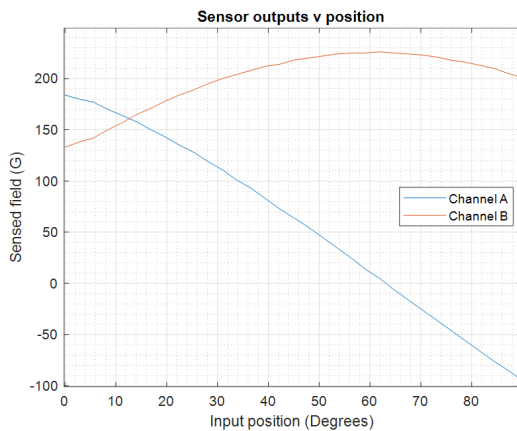


Figure 3: Sensed magnetic target.

Note the distorted shape of the top curve, as well as a gross offset.

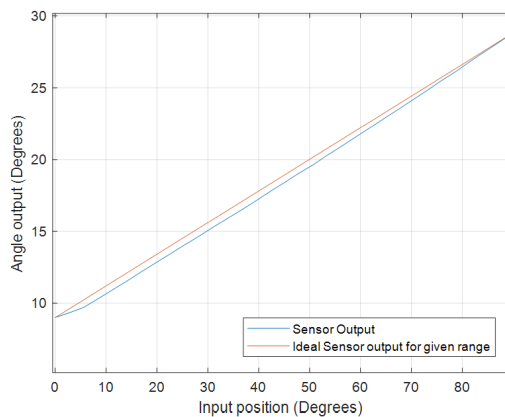


Figure 4: Reported angle output with the distorted inputs.

For the sensor to then reflect the position truthfully, it needs its own corrections.

The A31315 provides three layers of corrections to obtain the most accurate representation of the physical position of the module:

- Sensor gain and offset adjustments for each channel input (Including additional temperature coefficient options for more complex cases).
- Two-point correction of angle output to adjust starting point reporting and gain slope.
- Linearization up to 33 points to correct for non-linear imperfections.

### Fixing the Hall Sensor Gain and Offset

For the best performance, correcting gain and offset up front will have the greatest impact on performance later on.

To correct for the sensor data, one needs to model the sensed signals. This is typically easiest to do by finding

one signal that touches zero. For the signals in Figure 3, the bottom curve crosses zero at 30.36 degrees, but is not symmetric about this zero. The curve itself is descending, suggesting that it can be described with a cosine function. Therefore, the top curve is the complementary sine function.

There are numerous approaches to fitting the sensed curves to mathematical models of varying degrees of accuracy. With the goal being to find the angle of mechanical position, the signals should be kept simple to sine and cosine functions with amplitudes and offsets as the only variable to be found.

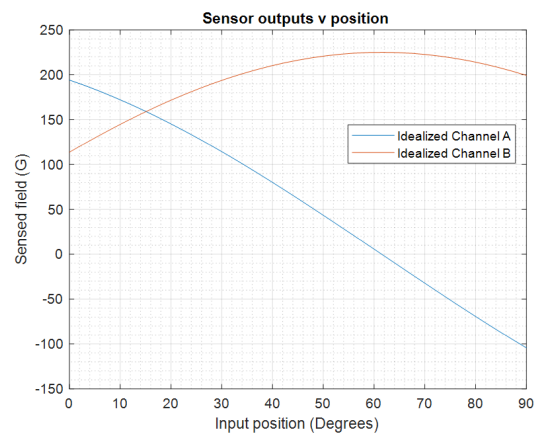


Figure 5: The modelled curves.

For this application, the use of curve-fitting found the inputs to be approximated as:

$$\text{Equation 1: } a(\theta) = 202 \cos(\theta + 0.53) \text{ [G]}$$

$$\text{Equation 2: } b(\theta) = 225 \sin(\theta + 0.53) \text{ [G]}$$

Numerically (by counts), Equation 1 and Equation 2 are described as:

$$\text{Equation 3: } a(\theta) = 6646 \cos(\theta + 0.53)$$

$$\text{Equation 4: } b(\theta) = 7373 \sin(\theta + 0.53)$$

In order to obtain the corrected gain and offset, there are four registers in the A31315 that handle these coefficients:

- Offs\_c\_a – adjusts the offset of channel A.
- Offs\_c\_b – adjusts the offset of channel B.
- Sens\_c\_a – adjust the sensitivity of Channel A.
- Sens\_c\_b – adjusts the sensitivity of channel B.

The default values are:

- Offs\_c\_<x> = 0 .
- Sens\_c\_<x> = 2048.

When using the A31315 Samples programming software, these registers are found in the EEPROM tab, shown in Figure 6.

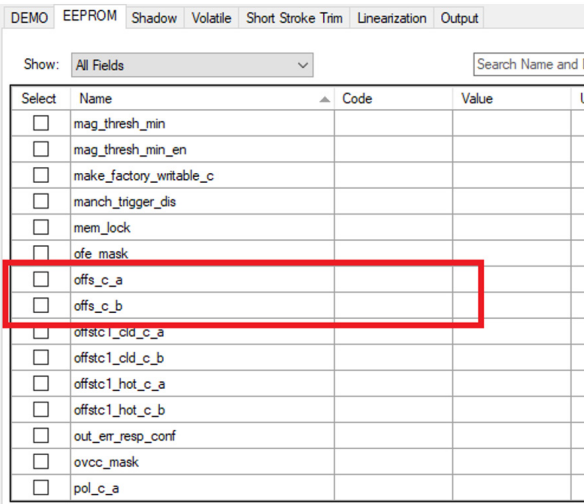


Figure 6: Offset registers in the A31315 Samples software.

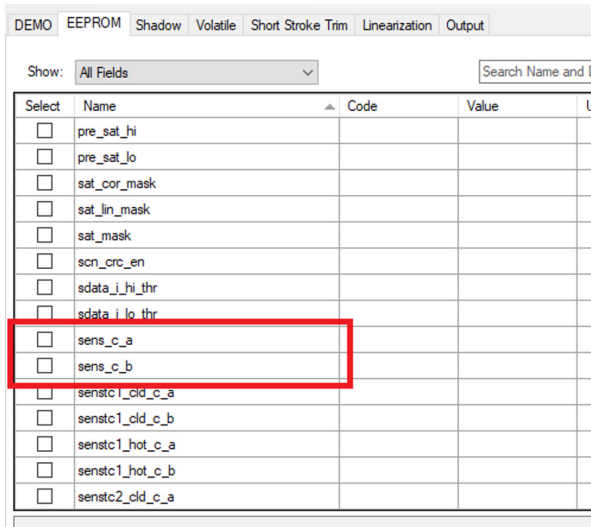


Figure 7: Sense registers within the Samples software.

Ultimately, the amplitudes should be equalized to achieve best results. In this case, with channel A, the sensitivity is less than the desired 225 G measured for channel B. So leveraging the sensitivity register, the sensitivity will be increased from 1 to 7373/6646 or 1.109.

Equation 5:  $sens\_c\_b = 1.109 \times 2048$

Equation 6:  $sens\_c\_b = 2048$  [default]

The sensitivity will affect the offset values, so gain should be corrected before considering offset adjustments. Restating equation 3:

Equation 7:  $a(\theta) = 7373 \sin(\theta + 0.53)$

In instances where an offset was needed, this would be adjusted after the gain adjustment of the front end. While the sensitivity is generally intuitive (2048 counts = 1, 1024 counts = 0.5, etc.), the offset registers are two bits smaller and additionally signed in nature, making every one count of offset equivalent to eight counts of output.

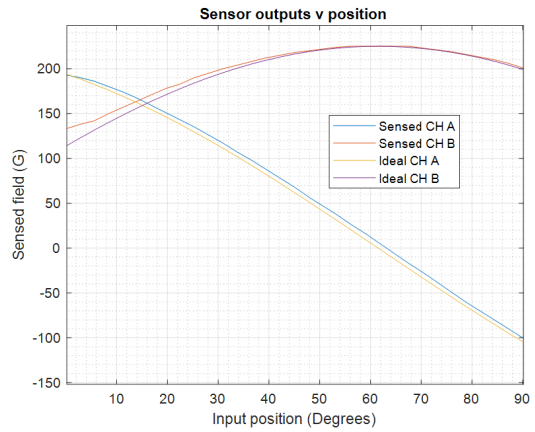


Figure 8: The ideal curves compared to the sensor with gain and offset applied. Note the nonlinear distortion in Channel A's output versus the ideal signal.

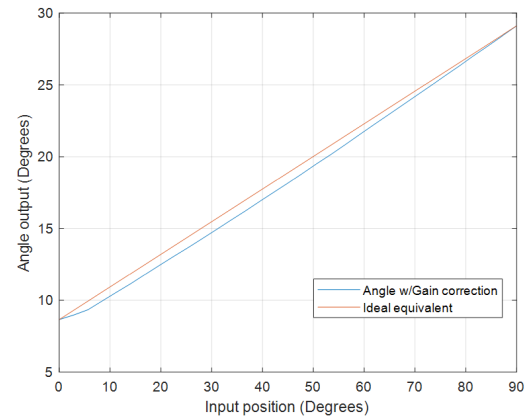


Figure 9: The resulting angle output reported by the sensor compared to the ideal angle output.

### Angle Gain and Offset Correction

For compliance to the feedback and control system, the sensor must output analog values from 0.5 to 4.5 V. Presently, the angle output provided would grant 0.166 to 0.458 V, hardly of value. Thus, an additional function is necessary to correct for this limited range. The A31315 offers a two-point programming block that will adjust the starting point of the output, as well as adjust the gain slope of the angle output.

There are two methods to program the coefficient and offset values in the two-point programming block:

- Register manipulation via:
  - Angle\_gain
  - Pre\_gain\_offset
- Semi-automatic via Samples Programming Software

### Register Manipulation

Performing the adjustments through register manipulation is straightforward and is easily calculated by hand. Relevant registers for this block are found within the “Short-Stroke” option of the dropdown menu within the EEPROM tab.

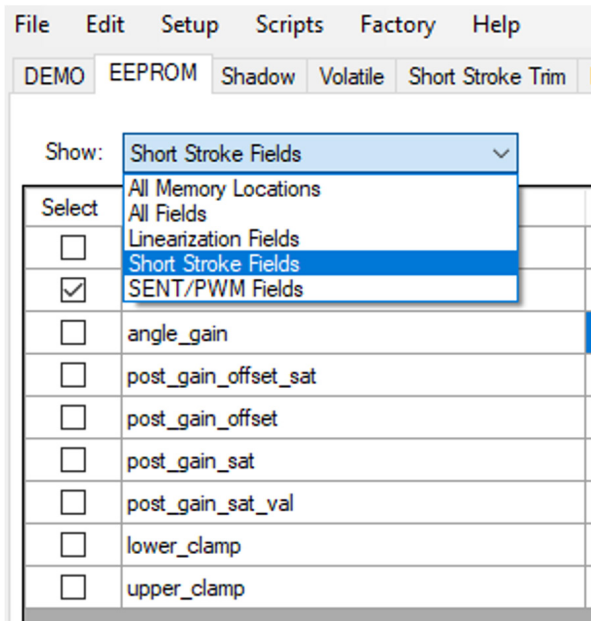


Figure 10: Two-point programming register group selection

Thus far, the plots have been expressed relative to the 90-degree rotation. The samples software operates on the assumption of 360° maximum and so will express results differently than have been shown so far.

Internally, the A31315 operates on a range of 0 to 65535 counts to represent the final angle. To set the zero point, an offset would be added to induce a rollover and reach a count of 0. However, when noise considerations are given, it is useful to add a small additional offset to overcome the noise. If the final value is 90 degrees, and

a small offset of 0.05 degrees is added, the offset can be found from the equation:

$$\text{Equation 8: } 90.05 = \text{current\_minimum} + \text{offset}$$

In the case of Figure 9, the minimum is around 11.5°, so:

$$\text{Equation 9: } 90.05 - 11.5 = 78.55$$

For the value to enter into the Code field (see Figure 11):

$$\text{Equation 10: } \text{Counts} = 78.55 / 90 \times 32768$$

$$\text{Equation 11: } \text{Counts} = 28599$$

Entering 28599 into the “code” field of the register table would populate the corresponding value field with 314.198°. This would be correct in applications that traverse the full 360°, and incidentally is the value four times the result of Equation 11.

Angle gain is just as easy to obtain; first find the present change of angle:

$$\text{Equation 12: } 34^\circ - 11.5^\circ = 22.5^\circ$$

Then find the maximum possible output angle:

$$\text{Equation 13: } \text{max\_angle} = 90 \times 65535 / 65536$$

$$\text{Equation 14: } \text{max\_angle} = 89.998$$

The needed gain is then:

$$\text{Equation 15: } \text{angle\_gain} = 89.998 / 22.5$$

$$\text{Equation 16: } \text{angle\_gain} = 3.9999$$

This value may be entered directly into the “value” field of the angle\_gain row within the software. This may be computed manually as:

$$\text{Equation 17: } \text{Angle\_gain} = 3.999 \times 1024$$

$$\text{Equation 18: } \text{Angle\_gain} = 4096$$

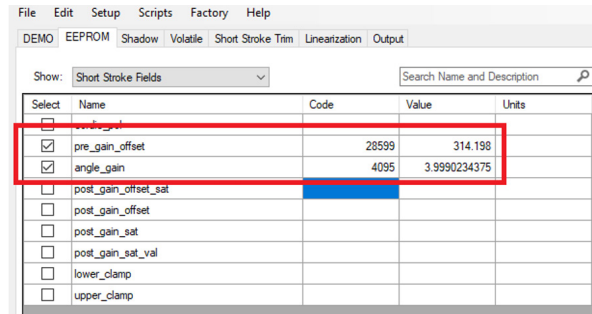


Figure 11: Manually processed two-point-programming values.

From the settings written to the two-point programming block, the new results are shown below:

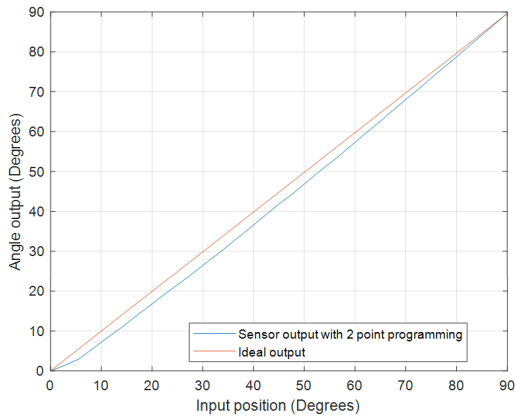


Figure 12: New angle output vs. input after two-point programming block.

It is at this time that angle error should be given attention. Figure 13 shows the angle error exhibited by the sensor.

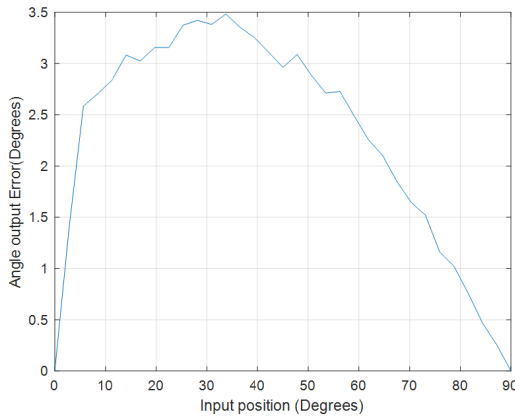


Figure 13: Angle error of the sensor with two-point programming applied.

### Linearization

The last step in tuning the A31315 is to correct for the angle errors of Figure 13.

The linearization engine of the A31315 can take 6 to 33 angle samples and perform a piecewise correction on the results.

For this example, only eight points will be leveraged as a good balance of accuracy and configuration time. Table 1 presents a list of true input position, to sensed position:

Table 1: Ideal position vs sensed output

Real Position	Sensed Position
0	0.00825
11.24983	8.3757
22.49965	19.25903
33.74948	30.13688
44.99933	41.86065
56.24915	53.30018
67.49898	65.38375
89.99863	89.63883

Table 2: Same values of Table 1, corrected to satisfy the software's requirements of range.

Real Position (corrected)	Sensed Position (corrected)
0	0.033
44.9993	33.5028
89.9986	77.0361
134.9979	120.5475
179.9973	167.4426
224.9966	213.2007
269.9959	261.535
359.9945	358.5553

These values may be entered directly or loaded from a file into the Linearization tab within the samples software.

**Note: Be mindful, as the software operates on 360° ranges, all values should be multiplied by 4 to be compliant with the software's expectation.**

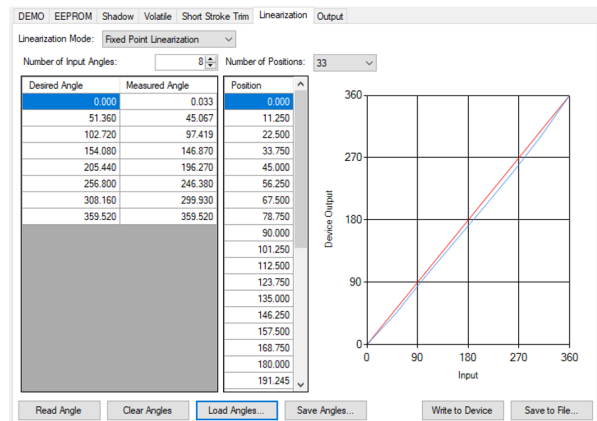


Figure 14: Linearization tab within the A31315 Samples Software.

In this case, a simple click of “Write to Device” computes the coefficients and programs the device. The new final result is shown in Figure 15.

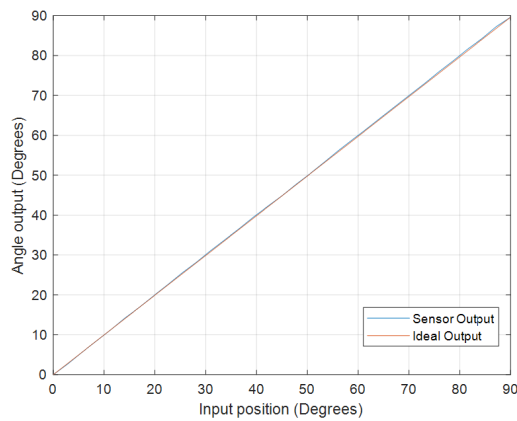


Figure 15: Linearized output of the sensor.

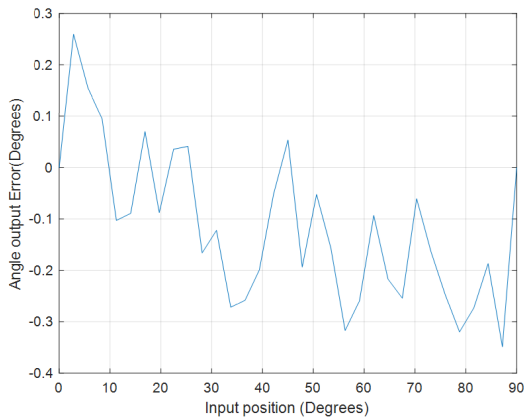


Figure 16: Angle output error post-linearization.

As Figure 16 illustrates, the angle error changed from a serious 3° down to 0.08° or less.

Thus, with the A31315, high accuracy is obtained in measuring the butterfly valve's true position for the feedback and control system.

Once the sensor has been tuned to the desired operating range, the final step is to configure the part to produce the intended output. In this application, correct output spans 0.5 to 4.5 V, leaving margins for wire-break detect or other diagnostic/error detecting. The A31315 includes output scaling through the register `be_scale`. For this particular application, setting `be_scale` to 6 compresses the output to within 0.5 V from either rail, granting the specified range. Figure 17 illustrates the analog output as a function of butterfly valve position.

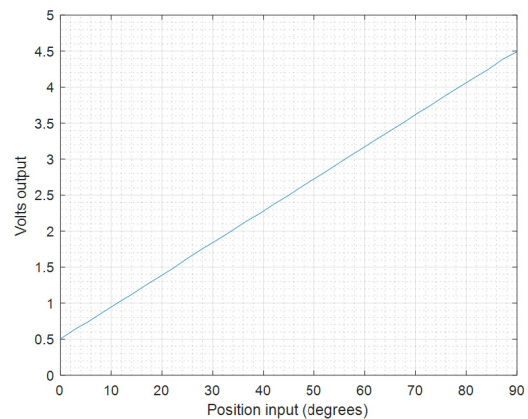


Figure 17: Analog Output as a function of butterfly valve position.

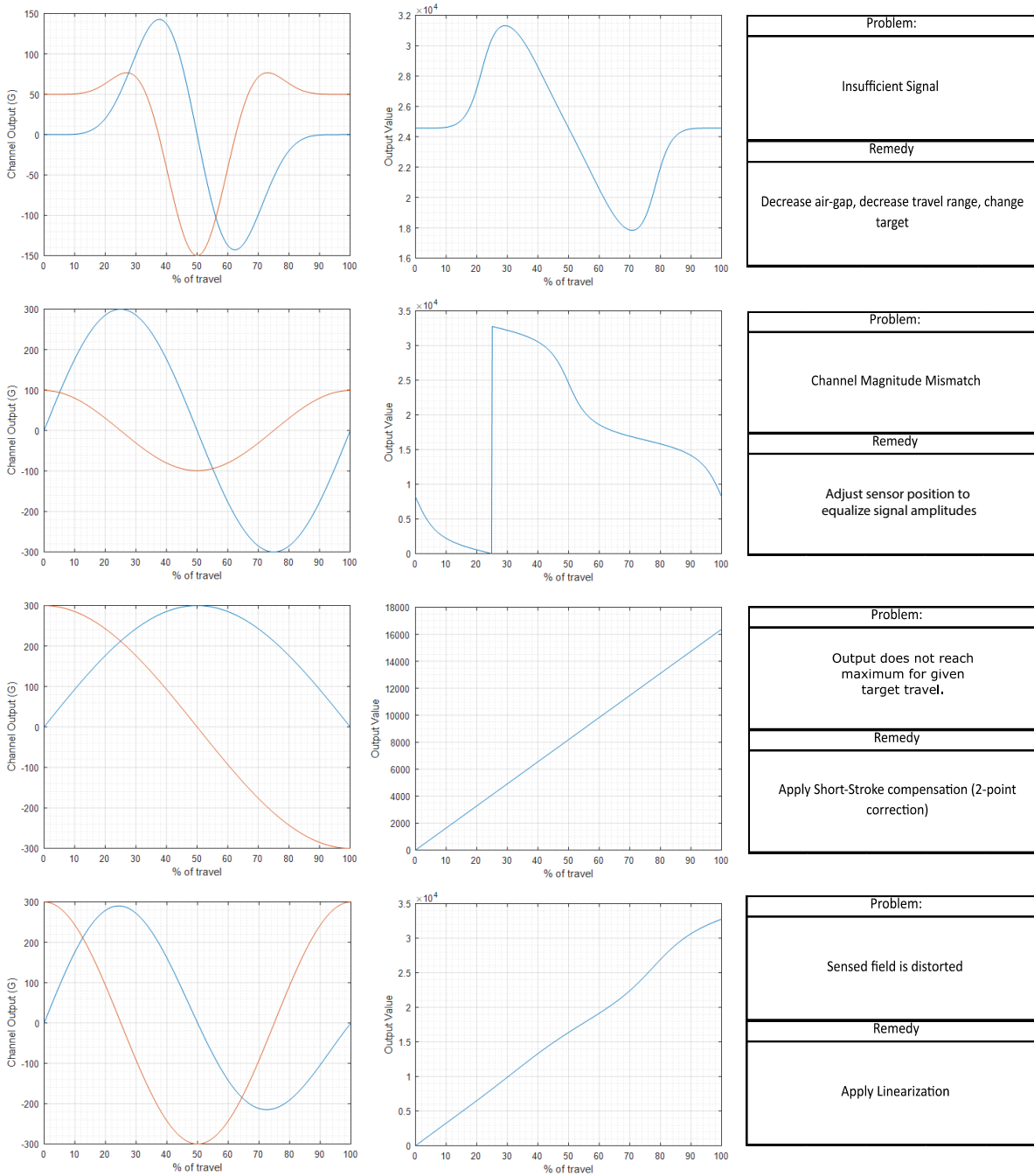


Figure 18. Problem and solution quick reference.

### Revision History

Number	Date	Description
–	September 21, 2020	Initial release
1	September 19, 2022	Minor editorial update (improved text spacing)

Copyright 2022, Allegro MicroSystems.

The information contained in this document does not constitute any representation, warranty, assurance, guaranty, or inducement by Allegro to the customer with respect to the subject matter of this document. The information being provided does not guarantee that a process based on this information will be reliable, or that Allegro has explored all of the possible failure modes. It is the customer's responsibility to do sufficient qualification testing of the final product to ensure that it is reliable and meets all design requirements.

Copies of this document are considered uncontrolled documents.